International Journal of Technology (2015) 4: 555-564
ISSN 2086-9614

SYNTHESIS OF LITHIUM TITANATE ($Li_4Ti_5O_{12}$) THROUGH HYDROTHERMAL PROCESS BY USING LITHIUM HYDROXIDE (LiOH) AND TITANIUM DIOXIDE (TiO_2) XEROGEL

Bambang Priyono[1*], Anne Zulfia Syahrial[1], Akhmad Herman Yuwono[1], Evvy Kartini[2], Mario Marfelly[1], Wahid Muhamad Furkon Rahmatulloh[1]

[1] *Department of Metallurgy and Materials Engineering, Faculty of Engineering, Universitas Indonesia, Kampus Baru UI Depok, Depok 16424, Indonesia*
[2] *Center for Science and Technology of Advanced Materials, BATAN, Puspiptek Serpong, Indonesia*

(Received: September 2015 / Revised: October 2015 / Accepted: October 2015)

ABSTRACT

Lithium Titanate ($Li_4Ti_5O_{12}$) or (LTO) has a potential as an anode material for a high performance lithium ion battery. In this work, LTO was synthesized by a hydrothermal method using Titanium Dioxide (TiO_2) xerogel prepared by a sol-gel method and Lithium Hydroxide (LiOH). The sol-gel process was used to synthesize TiO_2 xerogel from a titanium tetra-*n*-butoxide/Ti(OC_4H_9)$_4$ precursor. An anatase polymorph was obtained by calcining the TiO_2 xerogel at a low temperature, i.e.: 300^{o}C and then the hydrothermal reaction was undertaken with 5M LiOH aqueous solution in a hydrothermal process at 135^{o}C for 15 hours to form $Li_4Ti_5O_{12}$. The sintering process was conducted at a temperature range varying from 550^{o}C, 650^{o}C, and 750^{o}C, respectively to determine the optimum characteristics of $Li_4Ti_5O_{12}$. The characterization was based on Scanning Thermal Analysis (STA), X-ray Powder Diffraction (XRD), Field Emission Scanning Electron Microscopy (FESEM), Fourier Transform Infrared spectroscopy (FTIR), and Brunauer-Emmett-Teller (BET) testing results. The highest intensity of XRD peaks and FTIR spectra of the LTO were found at the highest sintering temperature (750^{o}C). As a trade-off, however, the obtained LTO/$Li_4Ti_5O_{12}$ possesses the smallest BET surface area (< 0.001 m^2/g) with the highest crystallite size (56.45 nm).

Keywords: Anode material; Hydrothermal; $Li_4Ti_5O_{12}$; Li-ion battery; Sintering; Sol-gel; TiO_2 xerogel

1. INTRODUCTION

Various ideas have been introduced to overcome the energy crisis and environmental pollution. The most promising one is development of an electric vehicle, which has zero emissions because the electric power to charge the car's battery comes from renewable energy sources. Electric vehicles would also create additional economic development opportunities by improving the quality of life, reducing energy spending, and decreasing reliance on foreign oil (Todd, 2013). The fuel tank of the electric car is now in the form of a rechargeable battery and the most widely used is a Lithium Ion Battery (LIB). In this LIB, graphite is commonly used as an anode material. During the intercalation process in the graphite anode, however, the formation of dendritic structures may cause short-circuits and volume expansion (Wang et al., 2013). It is also suffers from the formation of the Solid Electrolyte Interphase (SEI) that may

* Corresponding author's email: bambang.priyono@ui.ac.id, Tel. +62-21-7270078, Fax. +62-21-7270077
Permalink/DOI: http://dx.doi.org/10.14716/ijtech.v6i4.1965

lead to a decrease in specific energy capacity (Jiang et al., 2014). The solid electrolyte interphase (SEI) formation could be avoided by using a material having an insertion potential above the SEI formation potential (0.9V).

One of the promising candidates to replace graphite is LTO since LTO's insertion potential is at 1.55 V (1.55 V vs. Li/Li^+), which is well above the SEI formation potential (Maloney et al., 2012). Lithium titanate also offers some advantages. In this event, LTO has been known as a zero-strain insertion oxide (Mosa et al., 2012), it can experience thousands of cycles with little capacity loss and it is able to undergo fast charging (Wang et al., 2013). In addition, LTO has the potential for electrochemical reaction kinetics leading to excellent rate capability as well as stable cycling performance, due to its electrochemical characteristics (Li & Mao, 2014).

Lithium titanate has a major drawback, however, due to its low electrical conductivity (Mosa et al., 2012). Hence, there would be a need for an improvement, especially for use in high current applications. Although LTO possesses a theoretical specific capacity of 175 mAh/g, the capability of providing charge/discharge currents are relatively low due to its large polarization, resulting from low electrical conductivity (Mosa et al., 2012) and slow Li-ion diffusion (Ouyang et al., 2007). Some efforts to enhance LTO conductivity have already been carried out by doping with other elements (Zhang et al., 2014) and coatings using more conductive materials (Park et al., 2008). To increase the ionic diffusion of ion Li^+, the LTO particle size has been reduced to increase the surface contact between electrolyte and electrode, and also shorten the diffusion path of lithium ions and electrons as means to improve the lithiation kinetics (Zhang et al., 2013).

The sol-gel method has been applied extensively to synthesize nanoparticles due to its ability to control the reaction step at the molecular level and to attract nanoparticles with high homogeneity (Bilecka & Niederberger, 2010). The product resulting from the sol-gel process has the characteristics of a higher surface area when compared to the solid-state process (Priyono et al., 2013). The other advantage of the sol-gel method is that the sintering temperature required to form the structure of spinel-crystalline is significantly lower than that of the solid-state method (Zhang et al., 2013). This is due to most of the LTO being used as anode in the form of a *Fd3m* spinel structure (Wen, 2012).

The hydrothermal technique is a method used for reacting two or more compounds in the autoclave with the aid of water vapor pressure over 1 atm and temperatures above 100°C (Byrappa & Yoshimura, 2001). To improve the solid nanostructure, the hydrothermal process was aged at 80–240°C for 1–4 days, and this was reported to be able to increase the degree of crystallinity and thermal stability by minimizing the grain growth up to a temperature of 800°C (Wang & Ying, 1999).

In this work, LTO is synthesized using the sol-gel procedure to prepare TiO_2, followed by hydrothermal method combined with solution impregnation mixing and sintering to form the spinel structure of LTO. The whole process was aimed at obtaining LTO with nano-crystalline structures and crystallite sizes in the range of 10 to 100 nm to support its function as an anode material in a lithium-ion battery.

2. EXPERIMENTAL METHOD

Titanium tetra-*n*-butoxide/ $Ti(OC_4H_9)_4$ (Kanto Chemical), Ethanol/C_2H_5OH (pa), HCl 1M, and LiOH (pa) were used in this work. The sol-gel process is used to prepare TiO_2 xerogel. Firstly, titanium tetra-*n*-butoxide was used to prepare TiO_2 xerogel which was further calcined at 300ºC to obtain TiO_2 anatase. The procedure to obtain TiO_2 xerogel was explained in our previous work (Priyono et al., 2013). After xerogel was ground in mortar, the calcination was carried out at 300°C for 3 hours under the airflow to remove the remaining organic compounds and to

complete the formation of anatase TiO_2. The TiO_2 powder was obtained and then impregnated with aqueous LiOH (5M), and then further hydrothermally treated in a Teflon-lined autoclave at a temperature of 135ºC for 15 hours. Finally, the sintering process was carried out at temperatures varying from 550ºC, 650ºC and 750ºC, respectively to obtain ($Li_4Ti_5O_{12}$)/LTO. The off-white LTO powder was collected for further analysis.

The characterization by x-ray diffraction/XRD (Bruker AXS θ−2θ diffractometer, Philips PW3020) was carried out to identify the crystal structure of the obtained solid samples. The crystallite size was estimated based on XRD data via Scherrer's equation analysis. Furthermore, Brunauer-Emmet-Teller (BET) measurement (Quantachrome NOVA 1200e) was used to determine the surface area of the sample. FESEM analysis was performed to identify the surface morphology and particle size of LTO. Finally, FTIR (Shimadzu IR Prestige-21) analysis was carried out to verify the stretching bonds existing in the oxide network as a means to identify the functional groups contained in the compounds (Sui et al., 2006). For comparison purposes, the LTO obtained by the courtesy of the KIST (Korean Institute of Science and Technology) was used in this research as a reference.

3. RESULTS AND DISCUSSION

3.1. Agglomeration during Calcination

The BET surface area measurement showed that the anatase TiO_2 obtained via the sol-gel method and calcined at 300ºC has a surface area of 148.04 m^2/g, which is higher than that calcined at 420ºC (Priyono et al., 2013). The surface area of the synthesized TiO_2 xerogel in this work is significantly higher than those of commercial ones, i.e. from Merck (10 m^2/g) (Augugliaro et al., 2005) and Sigma (18.75 m^2/g) (Ruslimie et al., 2011). This confirms that the sol-gel method could synthesize a solid material with a high surface area (Wen, 2012). Thus, the present TiO_2 xerogel has a prospective as a better starting material for manufacturing the high surface area LTO. Analogically, to obtain high surface area LTO, it must use a high surface area starting material, since during the subsequent heat treatment process to obtain the crystalline structure, the agglomeration in the solid cannot be avoided, and thus reducing the surface area. In view of the foregoing, it is important to use the lower temperature process during calcination and sintering in order to preserve the surface area of the solid (Priyono et al., 2015).

3.2. Formation of Initial LTO Crystallite during Hydrothermal

The sample obtained after hydrothermal process appeared as light brown solid. The XRD pattern of the post-hydrothermal solid is depicted in Figure 1 and the FESEM image of post-hydrothermal solid is shown in Figure 2.

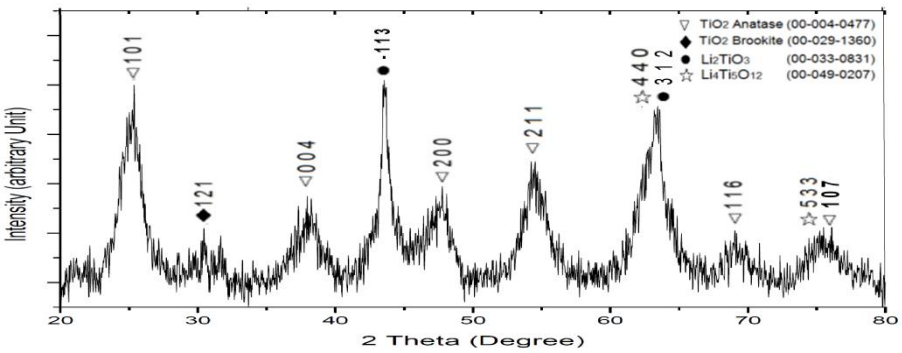

Figure 1 X Ray-Diffraction Pattern of anatase TiO_2 xerogel mixed with LiOH and hydrothermalled at 135ºC, 15 h

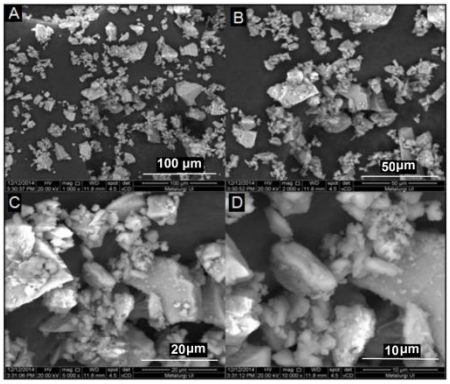

Figure 2 FESEM Micrograph of post-hydrothermal solid

From Figure 1, it can be seen that the diffraction pattern shows four compounds, *i.e.*: TiO_2 anatase, TiO_2 brookite, Li_2TiO_3 and $Li_4Ti_5O_{12}$. The peaks of Li_2TiO_3 and $Li_4Ti_5O_{12}$ are detected by software embedded in the XRD instrument (X'pert HighScore) with a low match value, indicating that at this stage, the crystallite seed of both compounds starts to grow. The reaction of precursors during hydrothermal treatment starts to form the Li_2TiO_3 and $Li_4Ti_5O_{12}$ compounds and the particular crystallite planes of both compounds come into existence, but the fully crystalline phase does not occur until the higher temperature. The crystallite planes begin to transform from the amorphous phase. Some of peaks of the compounds Li_2TiO_3 and $Li_4Ti_5O_{12}$ are almost overlapped, due to at the 2θ value their respective positions being very close, particularly at plane (440) of $Li_4Ti_5O_{12}$ and plane (312) of Li_2TiO_3. Based on these results, it is shown that by using xerogel TiO_2 and LiOH precursor, the seed of Li_2TiO_3 and $Li_4Ti_5O_{12}$ could be initiated after the hydrothermal process. This finding could improve the results obtained (Suzuki et.al., 2011; Zhang, Cao, et al., 2013) that the hydrothermal process cannot synthesize the lithium titanate directly, but after heat treatment the precursor is transformed to a spinel $Li_4Ti_5O_{12}$. The peak intensity of the TiO_2 anatase, Li_2TiO_3 and $Li_4Ti_5O_{12}$ compounds looks similar. The crystallite size calculated via Scherrer's equation by the Williamson-Hall Plot, using fit-size analysis is obtained equal to 15.7 nm.

The FESEM micrograph in Figure 2 shows the particles of the solid in the form of irregular agglomerates with a mean size of 1.79 µm is measured using ImageJ software. However, this value may not fully represent the real situation due to several larger-sized particles that were cut off during the image enlargement process in the instrument. The agglomeration of particles could be increased by the existence of moisture during the hydrothermal process (Hintz & Thomas, 2014).

3.3. Formation Spinel LTO during Sintering

The XRD pattern of the post-sintering solids together with LTO reference from KIST are shown in Figure 3. Furthermore, the average crystallite size of the solids is presented in Table 1.

Table 1 Average crystallite size diameter

Sintering Temperature (^oC)	Crystallite size (nm)
550	42.68
650	44.26
750	56.45

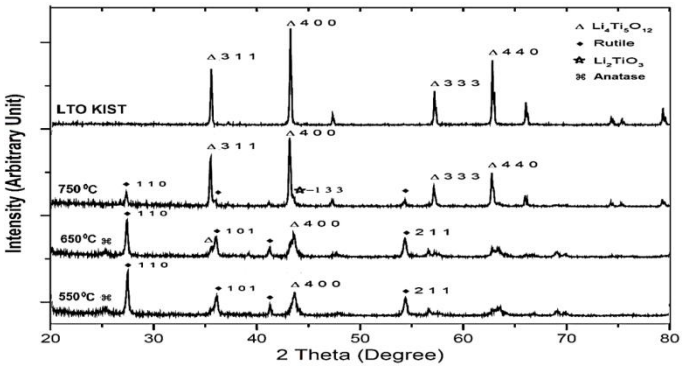

Figure 3 X Ray-Diffraction Pattern of the solid products sintered at temperatures 550ºC, 650ºC, and 750ºC, respectively

From Figure 3, it can be seen that the XRD patterns of the solids differ gradually at temperatures 550ºC, 650ºC and 750ºC, respectively. In the first finding, at temperature 550ºC, the TiO_2 rutile (JCPDS: 00-004-0551) peak intensity is the strongest, followed by LTO ($Li_4Ti_5O_{12}$) spinel crystalline structure (JCPDS: 00-049-0207) and a small TiO_2 anatase (JCPDS: 00-001-0562) peak at 25.3º. Then, at temperature 650ºC, the smaller TiO_2 anatase peak is still observed and TiO_2 rutile peak intensity is also getting lower than that of the reading at 550ºC, while the LTO peak looks stronger. Finally, the outcome of the sintering temperature at 750ºC is that the LTO reaches a major phase, and the rutile peaks are getting significantly lower. However, the small peak of Li_2TiO_3 (JCPDS: 01-071-2348) is detected at 43.6º. The above result shows that the increasing temperature in the range of 550ºC to 750ºC is in favor of LTO formation.

The rutile TiO_2 phase is present in all sintered products, since the sintering temperature is under 800ºC (Shin et al., 2012). If the sintering temperature is above 800ºC, it will result in grain growth and an increase in the particle size diameter, thus the agglomeration will be increased. The impurity of the TiO_2 rutile is formed by an unreacted TiO_2 anatase that occurs during the reaction formation of LTO. It is noted at the sintering temperature 750ºC result, the existence of peaks Li_2TiO_3 indicates that the unreacted TiO_2 anatase is caused not only by loss of the Li^+ ion source during sintering process, but also by an inhomogeneous mixture during the solid state mixing process. The presence of Li_2TiO_3 compound which has a molar ratio of Li/Ti greater than $Li_4Ti_5O_{12}$, shows that not all Li^+ ions react uniformly with the TiO_2 anatase thus it forms Li_2TiO_3 and a residual unreacted anatase TiO_2 that will transform into the rutile TiO_2 (Hong et al., 2012). Furthermore, the low intensity with an almost similar height of Li_2TiO_3 and TiO_2 rutile peaks at the stoichiometric composition indicates that there is a little loss of the Li^+ ion source during the sintering process.

The Li_2TiO_3 compound usually becomes one of the major impurities in the synthesizing process of the $Li_4Ti_5O_{12}$ compound. To have a condition of the single phase $Li_4Ti_5O_{12}$ free from impurities, such as Li_2TiO_3, is very difficult. As reported by Wen (Wen, 2012), Li_2TiO_3 always coexists as an impurity along with $Li_4Ti_5O_{12}$, which is obtained by the solid-state method. It is noticeable that both Li_2TiO_3 and $Li_4Ti_5O_{12}$ phases are structured in layers, far from perfect, with their interplanar distances, Li_2TiO_3 (002) and $Li_4Ti_5O_{12}$ (111), being very close to each other, i.e. 4.80Å and 4.84 Å, respectively. These two substances most probably interlock with each other, at the inception stage of their coexistence. Thus, by using a better mixing process of rutile-TiO_2 with a Li^+ ions source in a stoichiometric composition, the existence of an impurity, such as Li_2TiO_3 could be minimized.

As shown in Table 1, by using the Scherer equation with the Williamson-Hall fit size method calculation, data are obtained insofar as that the crystallite size of the solid sintered at 550ºC is 42.68 nm, at 650ºC is 44.26 nm, and at 750ºC is 56.45 nm, respectively, while the LTO KIST is 48.47 nm. The average crystallite size is bigger in accordance with the increasing sintering temperature. Thus, such an indication implies that this hydrothermal method using TiO_2 anatase prepared by the sol-gel method to produce LTO and the sintering temperature of 750ºC is sufficient to form the LTO/spinel crystalline, which is lower when compared to using TiO_2 anatase prepared from the solid state method as reported (Shin et al., 2012).

3.4. FTIR Spectra of LTO

The FTIR spectra of the xerogel TiO_2 are given in Figure 4. While the spectra of the all produced solids at the sintering temperatures of 550ºC, 650ºC, and 750ºC, respectively are presented in Figure 5.

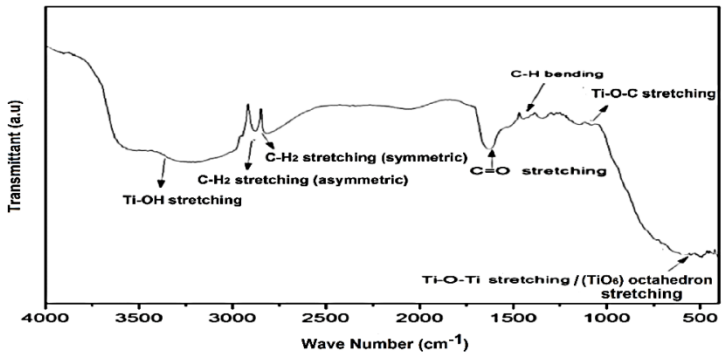

Figure 4 FTIR spectra of the xerogel TiO_2

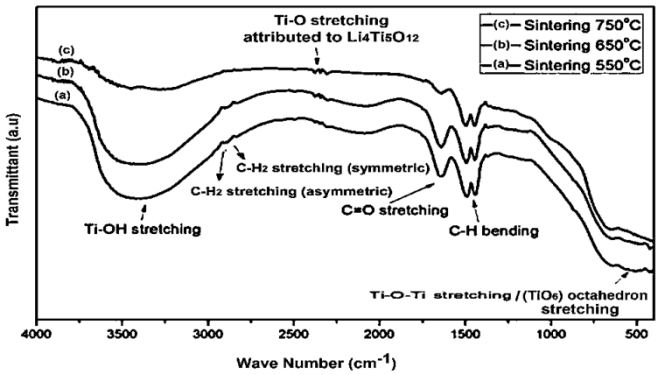

Figure 5 FTIR spectroscopy of the solid product sintered at temperatures 550ºC, 650ºC, and 750ºC

The results from the FTIR test of both xerogel TiO_2 and the sintered product of the LiOH and anatase TiO_2 mixture gives an indication of the LTO formation. Figure 4 indicates that the spectrum of the broad transmittant band, as is centered around 3,300 cm^{-1}, is attributed to stretching the vibrations of the hydroxyl group originating from Ti-OH (Vasconcelos et al., 2011). The other sources of the hydroxyl group in the present work are derived from the remaining water and alcohol in the xerogel. Additional peaks are then observed at 2,930 cm^{-1} (C-H_2 asymmetric stretching mode) and at 2,867 cm^{-1} (C-H_2 symmetric stretching mode) of the alcoxide. The band around 1,750–1,735 cm^{-1} is characteristic of the stretch vibration of the C=O bonds. The small peak at 1,343 cm^{-1} is a contribution from the C-H bending from the CH_3 group (Sui et al., 2006). There are also several small peaks at 1,132; 1,117; and 1,022 cm^{-1}, corresponding to Ti-O-C and the ending and bridging of the butoxyl groups of the alcoxide,

respectively. The oxo bonds can be observed by the presence of wide bands below 800 cm^{-1} (Sui et al., 2006). Such oxo bonds come from Ti-O-Ti and TiO_6 octahedron stretching.

As depicted in Figure 5, the result of FTIR in relation to the sintered product shown is that the spectrum around 2,300 cm^{-1} prevails, which becomes stronger in line with an increase in the sintering temperature. The process during sintering when a Li^+ source reacts with TiO_2 could be described as the migration of lithium ion into the nano-structure of TiO_2 to form LTO ($Li_4Ti_5O_{12}$) and such a process is enhanced by increasing of the sintering temperature at a range from 550ºC to 750ºC. The results above are in agreement with the XRD analysis. Therefore, the $Li_4Ti_5O_{12}$ compound has two absorption peaks at 2,359.7 cm^{-1} and 668.3 cm^{-1}, respectively, which are assigned to the stretching vibration of the Ti-O bond and MO_6 (TiO_6) octahedron, (Yan et al., 2012).

The FTIR sintered product result indicates that all spectra belong to the hydroxyl group made from Ti-OH, water and alcohol, the C-H_2 asymmetric stretching mode and the C-H_2 symmetric stretching mode of the alcoxide, which are getting lower and almost disappear at the sintering temperature 750ºC. The other spectra, such as the band around 1,750–1,735 cm^{-1} of the C=O bonds, the peak at 1,343 cm^{-1} of the C-H bending from the CH_3 group and several peaks at 1,132; 1,117; and 1,022 cm^{-1}, respectively from Ti-O-C are also decreasing in the same manner by the sintering temperature increase. This decreasing of the peaks is caused by decomposition of the related groups in the solid due to the raised temperature and the presence of the least residual organic compounds that were found at the highest sintering temperature.

3.5. Dense Particulate Formed during Sintering

The SEM results for all the produced sintering samples of the solids at the sintering temperatures of 550ºC, 650ºC, and 750ºC, respectively are shown in Figure 6. While, the results of the BET surface area testing of the sintered products are presented in Table 2.

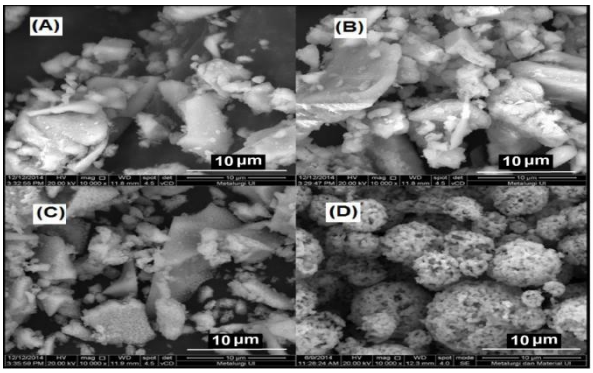

Figure 6 FESEM micrographs of post-sintering solid sintered at 550ºC (A), 650ºC (B), 750ºC (C), and LTO from KIST (D)

Table 2 BET surface area of the sintered product

Temperature (ºC)	Surface Area (m^2/g)
550	1.72
650	<0.001
750	<0.001

From Figure 6, it can be seen that particles with various shapes and sizes sticking together formed an irregular, flaky agglomerate. This is because the grain bonding and particle growth

during the hydrothermal process and the subsequent sintering process then formed a dense particulate. All these mechanisms lead to a low surface area, as shown in Table 2 above. The solid agglomerates of all products with a size bigger than LTO KIST are shown in Figure 6(D).

The magnificent image of Figure 6(D) showing tiny particles with a high level of homogeneity in size and shape is LTO from KIST, which is composed of a porous sphere agglomeration. This structure leads to the surface area being much higher than when compared to LTO from the present work. Therefore, it is suggested that the surface templating method could be an interesting way to improve the product. Furthermore, the density of the agglomerates and the low surface area of the solids also suggest that the mixing and hydrothermal processes of the TiO_2 anatase with a Li^+ ion source through aqueous solution LiOH impregnation method is not optimal, although the desired LTO is readily obtained.

4. CONCLUSION

The lithium titanate ($Li_4Ti_5O_{12}$)/LTO has been successfully synthesized using a hydrothermal method of TiO_2 xerogel prepared by the sol-gel method and lithium hydroxide with a calcination temperature at 300ºC to form the TiO_2 anatase and a sintering temperature at 750ºC to obtain the $Li_4Ti_5O_{12}$/spinel structure. The XRD-pattern shows all of the structures are readily crystallized. The loss of the Li^+ source during processing is not superfluous, indicating that this TiO_2 xerogel and LiOH mixture by a hydrothermal process could initiate the reaction to form $Li_4Ti_5O_{12}$ and could prevent the significant loss of the Li^+ source.

The effect of the sintering temperature at the range from 550ºC to 750ºC shows that the highest intensity of the XRD peaks and FTIR spectra attributed to the LTO were found at the highest sintering temperature. Finally, the high content of LTO ($Li_4Ti_5O_{12}$) obtained with the spinel crystalline structure at the sintering temperature of 750ºC is the optimum result to be used as an active material in making the anode for the Li-ion battery in further research. Finally, it is expected that such a material will have the necessary performance level when compared to graphite.

5. ACKNOWLEDGEMENT

The authors would like to thank the Hibah Pasca DRPM-UI (Directorate Research and Community Services Universitas Indonesia) 2015 grant awarded under contract No: 1727/UN2.R12/HKP.05.00/2015 for its financial support in relation to this research.

6. REFERENCES

Augugliaro, V., Coluccia, S., García-López, E., Loddo, V., Marcì, G., Martra, G., Palmisano, L., Schiavello, M., 2005. Comparison of Different Photocatalytic Systems for Acetonitrile Degradation in Gas–solid Regime. *Topics in Catalysis*, Volume 35 (3–4), pp. 237–244

Bilecka, I., Niederberger, M., 2010. New Developments in the Nonaqueous and/or non-Hydrolytic Sol–gel Synthesis of Inorganic Nanoparticles. *Electrochimica Acta*, Volume 55 (26), pp. 7717–7725

Byrappa, K., Yoshimura, M., 2001. *Handbook of Hydrothermal Technology, A Technology for Crystal Growth and Materials Processing*

Hintz, W., Thomas, J., 2014. Mechanical Process Engineering–Particle Technology Agglomeration. Book Section. In*: Universitat Magdeburg*

Hong, C.H., Noviyanto, A., Ryu, J.H., Kim, J., Yoon, D.H., 2012. Effects of the Starting mMaterials and Mechanochemical Activation on the Properties of Solid-state Reacted $Li_4Ti_5O_{12}$ for Lithium ion Batteries. *Ceramics International*, Volume 38 (1), pp. 301–310

Jiang, Z., Li, C., Hao, S., Zhu, K., Zhang, P., 2014. An Easy Way for Preparing High Performance Porous Silicon Powder by Acid Etching Al-Si Alloy Powder for Lithium Ion Battery. *Electrochimica Acta*, Volume 115, pp. 393–398

Li, X., Mao, J., 2014. Sol-hydrothermal Synthesis of $Li_4Ti_5O_{12}$/rutile-TiO_2 Composite as High Rate Anode Material for Lithium Ion Batteries. *Ceramics International*, Volume 40 (8), pp. 13553–13558

Maloney, R.P., Kim, H.J., Sakamoto, J.S., 2012. Lithium Titanate Aerogel for Advanced Lithium-Ion Batteries. *Applied Material & Interfaces*, Volume 4, pp. 2318–2321

Mosa, J., Vélez, J.F., Lorite, I., Arconada, N., Aparicio, M., 2012. Film-shaped Sol-gel $Li_4T_5O_{12}$ Electrode for Lithium-ion Microbatteries. *Journal of Power Sources*, Volume 205, pp. 491–494

Ouyang, C.Y., Zhong, Z.Y., Lei, M.S., 2007. Ab Initio Studies of Structural and Electronic Properties of $Li_4Ti_5O_{12}$ Spinel. *Electrochemistry Communications*, Volume 9 (5), pp. 1107–1112

Park, K., Benayad, A., Kang, D., Doo, S., 2008. Nitridation-driven Conductive $Li_4Ti_5O_{12}$ for Lithium Ion Batteries. *Journal of American Chemical Society Communication*, pp. 14930–14931

Priyono, B., Syahrial, A.Z., Yuwono, A.H., Kartini, E., Jodi, H., Johansyah, Wahid, M.F.R., 2015. Manufacturing Lithium Titanate ($Li_4Ti_5O_{12}$) by Addition of Excess Lithium Carbonate (Li_2CO_3) in Titanium Dioxide (TiO_2) Xerogel. In: *Proceedings of the 14th International Conference on Quality in Research (QiR) 2015, Faculty of Engineering, University of Indonesia*, pp. 2–7

Priyono, B., Yuwono, A.H., Munir, B., Rahman, A., Maulana, A., Abimanyu, H., 2013. Synthesis of Highly-ordered TiO_2 through CO_2 Supercritical Extraction for Dye-sensitized Solar Cell Application. *Advanced Materials Research*, Volume 789, pp. 28–32

Ruslimie, C.A., Razali, H., Khairul, W.M., 2011. Catalytic Study on TiO_2 Photocatalyst Synthesised via Microemulsion Method on Atrazine. *Sains Malaysiana*, Volume 40(8), pp. 897–902

Shin, J.W., Chung, K.Y., Ryu, J.H., Park, I.W., Yoon, D.H., 2012. Effects of Li/Ti Ratios on the Electrochemical Properties of $Li_4Ti_5O_{12}$ Examined by Time-resolved X-ray Diffraction. *Applied Physics A*, Volume 107, pp. 769–775

Shin, J.W.W., Hong, C.H.H., Yoon, D.H.H., 2012. Effects of TiO_2 Starting Materials on the Solid-state Formation of $Li_4Ti_5O_{12}$. *Journal of the American Ceramic Society*, Volume 95(6), pp. 1894–1900

Sui, R., Rizkalla, A.S., Charpentier, P.A., 2006. FTIR Study on the Formation of TiO_2 Nanostructures in Supercritical CO_2. *J. Phys. Chem. B*, Volume 110, pp. 16212–16218

Suzuki, S., Miyama, M., 2011. Microstructural Controls of Titanate Nanosheet Composites Using Carbon Fibers and High-rate Electrode Properties for Lithium Ion Secondary Batteries. *Journal of Power Sources*, Volume 196 (4), pp. 2269–2273

Todd, J., 2013. Analysis of the Electric Vehicle Industry Creating the Clean Energy Economy. *International Economic Development Council*, pp. 1–100

Vasconcelos, D.C.L., Costa, V.C., Nunes, E.H.M., Sabioni, A.C.S., Gasparon, M., Vasconcelos, W.L., 2011. Infrared Spectroscopy of Titania Sol-gel Coatings on 316L Stainless Steel. *Materials Sciences and Applications*, Volume 02 (10), pp. 1375–1382

Wang, C.-C., Ying, J.Y., 1999. Sol-gel Synthesis and Hydrothermal Processing of Anatase and Rutile Titania Nanocrystals. *Chemical Materials*, Volume 11(19), pp. 3113–3120

Wang, J., Zhao, H., Wen, Y., Xie, J., Xia, Q., Zhang, T., Zeng, Z., Du, X., 2013. High Performance $Li_4Ti_5O_{12}$ Material as Anode for Lithium-ion Batteries. *Electrochimica Acta*, Volume 113, pp. 679–685

Wen, R., 2012. Nanostructured $Li_4Ti_5O_{12}$ as Anode Material for Lithium Ion Batteries. *Master Thesis*. Faculty of Science, The University of New South Wales

Yan, H., Zhu, Z., Zhang, D., Li, W., Qilu, 2012. A New Hydrothermal Synthesis of Spherical Li4Ti5O12 Anode Material for Lithium-ion Secondary Batteries. *Journal of Power Sources*, Volume 219, pp. 45–51

Zhang, C., Zhang, Y., Wang, J., Wang, D., He, D., Xia, Y., 2013. $Li_4Ti_5O_{12}$ Prepared by a Modified Citric Acid Sol-gel Method for Lithium-ion Battery. *Journal of Power Sources*, Volume 236, pp. 118–125

Zhang, Y., Zhang, C., Lin, Y., Xiong, D., Wang, D., Wu, X., He, D., 2014. Influence of Sc^{3+} Doping in B-site on Electrochemical Performance of $Li_4Ti_5O_{12}$ Anode Materials for Lithium-ion Battery. *Journal of Power Sources*, Volume 250, pp. 50–57

Zhang, Z., Cao, L., Huang, J., Wang, D., Wu, J., Cai, Y., 2013. Hydrothermal Synthesis of $Li_4Ti_5O_{12}$ Microsphere with High Capacity as Anode Material for Lithium ion Batteries. *Ceramics International*, Volume 39 (3), pp. 2695–2698